Renewable Energy 115 (2018) 411–422

Contents lists available at ScienceDirect

Renewable Energy

journal homepage: www.elsevier.com/locate/renene

A novel soft computing model (Gaussian process regression with K-fold cross validation) for daily and monthly solar radiation forecasting (Part: I)

Abbas Rohani [a, *], Morteza Taki [b], Masoumeh Abdollahpour [a]

[a] Department of Biosystems Engineering, Faculty of Agriculture, Ferdowsi University of Mashhad, Iran
[b] Department of Agricultural Machinery and Mechanization, Ramin Agriculture and Natural Resources University of Khuzestan, Mollasani, Ahwaz, Iran

ARTICLE INFO

Article history:
Received 8 May 2017
Received in revised form
31 July 2017
Accepted 23 August 2017
Available online 26 August 2017

Keywords:
Global solar radiation
Sensitivity analysis
K-fold crosses validation

ABSTRACT

The main objective of this paper is to present Gaussian Process Regression (GPR) as a new accurate soft computing model to predict daily and monthly solar radiation at Mashhad city, Iran. For this purpose, metrological data was collected from Iranian Meteorological Organization for Mashhad city located at the North-East for the period of 2009–2014. All the collected data include of maximum, minimum and average daily outdoor temperature (T_{max}, T_{min} and T_{ave}), daily relative outdoor humidity (Rh), daily sea level pressure (p), day of a year (N), sunshine hours (N_s), daily extraterrestrial radiation on horizontal surface (H_0) and daily global solar radiation on horizontal surface (H). Results of sensitivity analysis showed that (N/Ns, T_{ave}, Rh, H_0) is the best data set group for evaluation of daily global solar radiation at this region. For the GPR model, MAPE, RMSE and EF were 1.97%, 0.16 and 0.99, respectively. Monthly evaluation showed that the main model is not suitable for every month, so for every month, perfect model was trained and tested. Generalizability and stability of the GPR model was evaluated by different sizes of training data with *5-fold* analysis. The results showed that GPR model can use with small size of data groups.

1. Introduction

The most important source of energy for the earth is the sun. The whole of life relays on the sun's energy. It is the main source for the chemical and biological processes on the earth. Also, it is the most environmentally friendly form of all energies, it can be used in many ways, and it is suitable for all social systems [1]. When we want to use the solar energy, accurate knowledge of solar radiation is needed as the first step and helps as the main input for different solar energy applications [2]. In some countries such as Iran and other developing countries, solar radiation instruments are not always available because of the high cost, need the equipment calibration and maintenance requirements, so different solar radiation models have been developed to estimate solar radiation [3–5]. Many solar radiation models are proposed to estimate solar radiation by difficult or simple techniques based on different sources of data such as meteorological, geographical, geostationary satellite images, artificial intelligent, time series, physically transfer and stochastic weather methods [6–19].

Many studies have been performed to investigate the applicability of different solar models in predicting the solar radiation at any locations. Razmjoo et al. [20], applied the Angstrom-Prescott (A-P) method for estimating the monthly global solar radiation in Ahvaz and Abadan cites, Iran. Results showed that the average amount of solar radiation annually is about 8.42 and 8.26 h for Abadan and Ahvaz cities, respectively. Moreover, constant equation coefficients were obtained as 0.30 and 0.49 for Abadan and 0.31 and 0.47 for Ahvaz city. The conclusion of this paper showed that the Khuzestan Province (south region of Iran) has a high potential of solar energy for investing. In another research, Adaptive Neuro-Fuzzy Inference System (ANFIS) was used to select the main factors which affect the solar radiation estimation [21]. In this study, four parameters were used to predict the solar radiation including mean sea level (MSL), dry-bulb temperature (DBT), wet-bulb temperature (WBT) and relative humidity (RH). The results showed that the DBT and RH are the main factors for the solar radiation prediction. Kumar et al. [22], compared the Artificial Neural Network (ANN) with Multiple Regression Models (MLR) to predict

* Corresponding author.
E-mail address: arohani@um.ac.ir (A. Rohani).

http://dx.doi.org/10.1016/j.renene.2017.08.061
0960-1481/

the monthly solar radiation. The results showed that ANN has the better performance values than the MLR model. The Mean Absolute Percent Error (MAPE) values of the ANN models are lower than those of the MLR models. In addition, the coefficient of correlation (R) values of the ANN are higher than those of MLR models. Mohanty et al. [23], reviewed the application of solar radiation models with soft computing and conventional approach for estimating the total global solar radiation. In this research, the authors classified all the models into two categories: empirical models and soft computing approach. The soft computing approach has three sessions: ANN, ANFIS and Radial Basis Function Network (RBFN). The authors had reviewed over than 110 researches and then concluded than soft computing model gives good accuracy by minimizing the error. Quej et al. [24], developed a new empirical model and predict the daily global solar radiation at six stations in Mexico. Results showed that the new developed model has the best correlation for all stations. Models based on temperature, rainfall and air humidity performed better than models that used temperature data only. This research concluded that the new propose model can be used in hydrologic and agricultural studies to estimate global solar radiation in warm sub-humid regions when temperature, precipitation and humidity data are available. A lot of researches developed or improved some of empirical or soft computing models to predict horizontal daily or monthly solar radiation [25–37]. Fig. 1 summarizes the flow charts of mainly used modeling techniques. According to above literature, the main goal of this paper is to application of Gaussian Process Regression (GPR) model as a new technique in this subject to predict daily and monthly global solar radiation and also evaluation this model with k-fold method. So the results of this model and its evaluation can use very simply for any thermal and solar systems (such as solar cells, solar collectors, solar stills, solar desalination, solar PV/T and others) analysis.

2. Material and methods

2.1. Study area and data collection

Mashhad is the second-largest metropolis of Iran and it is the capital of Razavi Khorasan province and has been located in north eastern Iran. Mashhad has been situated in longitude from 59°35E to 59°35E and latitude from 36°14N to 36°48N. This city is about 315 km^2 and its population according to the last census is 2,766,258 people. Fig. 2 shows the location of Mashhad city in Iran. Mashhad features a steppe climate (Köppen *BSk*) with hot summers and cool winters [38]. This city only sees about 250 mm (9.8 inches) of precipitation per year, some of which occasionally falls in the form of snow. Mashhad also has wetter and drier periods with the bulk of the annual precipitation falling between the months of December and May. Summers are typically hot and dry, with high temperatures sometimes exceeding 35 °C (95 °F). Winters are typically cool to cold and somewhat damper, with overnight lows routinely dropping below freezing. Mashhad enjoys on average just above 2900 h of sunshine per year. As the city is located in sunny region of Iran, it enjoys significant solar energy potential during the entire year.

In this study, the data were collected from the Iranian Meteorological Organization (IMO) for Mashhad city for the period of 2009–2014. This data include 8 parameters:

i. T_{ave}: Daily average outdoor temperature (°C)
ii. T_{max}: Daily maximum outdoor temperature (°C)
iii. T_{min}: Daily minimum outdoor temperature (°C)
iv. H: Daily global solar radiation on horizontal surface (KWh. $M^{-2}.d^{-1}$)
v. p: Daily sea level pressure (mbar)
vi. Rh: Daily relative humidity (%)
vii. H_0: Daily extraterrestrial radiation on horizontal surface (KWh. $M^{-2}.d^{-1}$)
viii. (N/N_s): is the corresponding sunshine duration, N is the hours of bright sunshine (day length) and Ns is the maximum possible duration of sunshine duration

The precision of the predictive models is mainly influenced by the quality of raw data utilized. The data cleaning procedure generally aims at enhancing the data quality by checking and filtering them from any uncertainty or erroneous.

2.2. An overview of Gaussian process regression

GPR works under the probabilistic regression framework, which takes as input a training data set $D = \{(y_n, x_n), \quad n = 1, 2, 3, \ldots, N\}$ of N pairs of vector input $x_n \in R^L$ and noisy scalar output y_n, and constructs a model that generalizes well to the distribution of the output at unseen input locations. The noise in the output models uncertainty due to factors external to x, such as truncation or observation errors. Here we assume that noise is additive, zero-mean, stationary and normally distributed, such that:

$$y = f(x) + \varepsilon, \quad \varepsilon \approx N\left(0, s^2_{\text{noise}}\right) \tag{1}$$

where s^2_{noise} is the variance of the noise [39]. The primary idea behind GPR is to use a Gaussian process (GP) to represent f, referred to as latent variables. The input x plays the role of indexing these latent variables such that any finite collection $\{f(x_1), \ldots, f(x_k)\}$ with unique indices follow a consistent Gaussian distribution. In this way, we limit ourselves to only looking at functions whose values correlate with each other in a Gaussian manner. In Bayesian framework, this is equivalent to putting a GP prior over functions. Due to the consistency requirement, we are able to make inference on function values corresponding to unseen inputs conveniently using a finite set of training data. A major advantage for using the Gaussian prior assumption is that functions can be conveniently specified by a mean function m(x) and a covariance function $k(x, x')$:

$$\begin{aligned} &m(x) = E[f(x)], \\ &k(x, x') = E[(f(x) - m(x))(f(x') - m(x'))] \end{aligned} \tag{2}$$

where $E[\cdot]$ denotes expectation. The form of the mean function is important only in unobserved region of the input space and usually set to zero. The properties of the process are then entirely dictated by the covariance function, which is by definition symmetric and positive semi-definite when evaluated at any pair of points in the input space [40].

The covariance function typically contains a number of free parameters called hyper parameters which define the prior distribution on f(x). The most commonly used is the squared exponential covariance function:

$$k(x, x') = q_1 exp\left(\frac{\|x - x'\|}{2q_2}\right) \tag{3}$$

where, $\|\cdot\|$ is a norm defined on the input space. Note that this covariance function decays rapidly when evaluated at increasingly distant pairs of input x and x', indicating weak correlations between f(x) and $f(x')$. (q_1) is a hyper parameter specifying the maximum allowable covariance. (q_2) is a strictly positive hyper parameter defining rate of decay in correlation as points become farther away from each other. Another hyper parameter (q_3) which is not

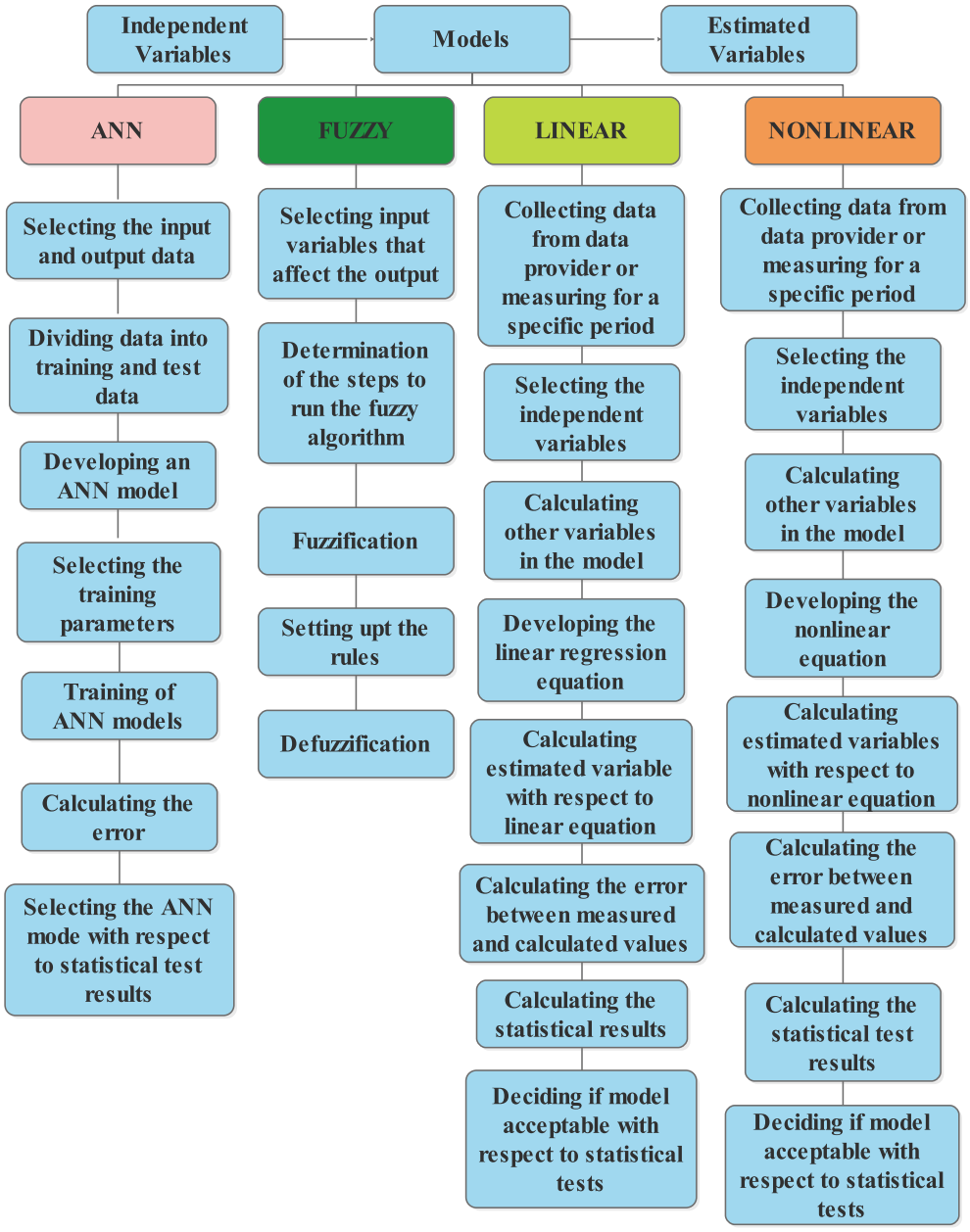

Fig. 1. Flowcharts of the models to estimate global solar radiation [18].

expressed explicitly in (Eq. (3)), is used to represent the unknown variance s^2_{noise} of Eq. (1). The hyper parameters $\{q_1, q_2, q_3\}$ are grouped together as a vector (q) treated as the realization of a random vector (Q). The realization that is most coherent with the data set is selected using training data and then used to make predictions [38].

2.2.1. Prediction with GPR

Assuming that the hyper parameters are known, inference is easily made. Denoting the vector of training latent variables by f and the vector of test latent variables by f^* we have the following joint Gaussian distribution:

$$p(f, f^*) = N\left(0, \begin{bmatrix} K_{f,f} & K_{*,f} \\ K_{f,*} & K_{*,*} \end{bmatrix}\right) \quad (4)$$

K is the symmetric covariance matrix whose *ijth* entry is the covariance between the *ith* variable in the group denoted by the first subscript and the *jth* variable in the group denoted by the second subscript (* is used in place of f^* for short), computed using covariance function $k(.,.)$ in Eq. (3) and corresponding hyper parameters [39].

2.3. K-fold cross validation

Cross-validation is a measurement of assessing the performance of a predictive model, and statistical analysis will generalize to an independent dataset. There are many types of cross-validation, such as repeated random sub-sampling validation, *K*-fold cross-validation, $K \times 2$ cross-validations, leave-one-out cross-validation and so on (Fig. 3).

In this study, we pick up *K*-fold cross-validation for selecting

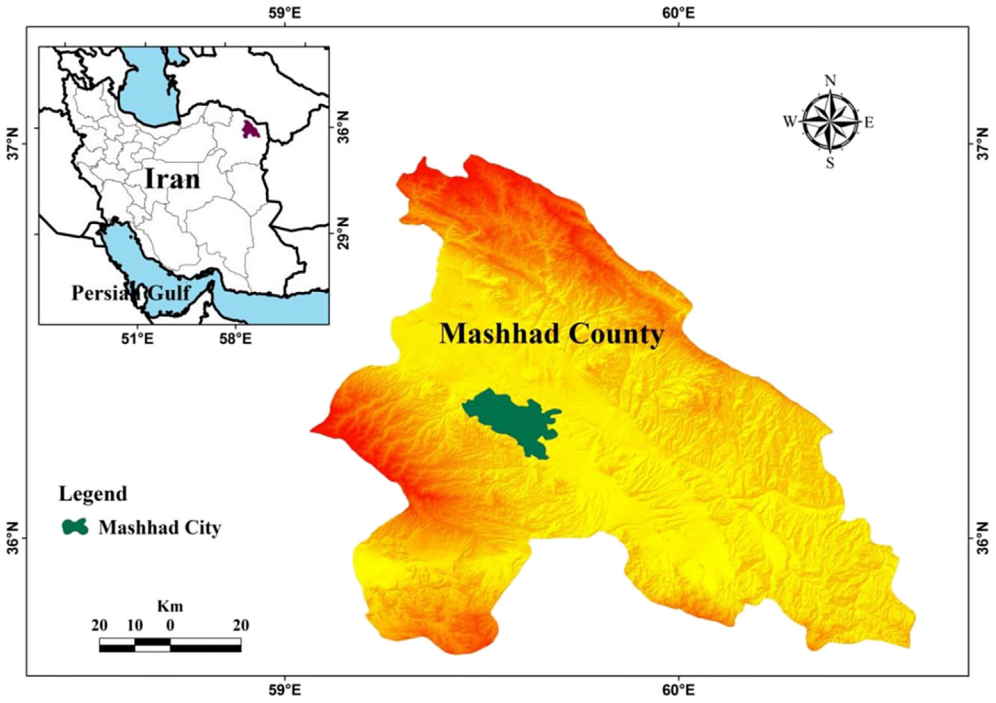

Fig. 2. Study area (Mashhad city).

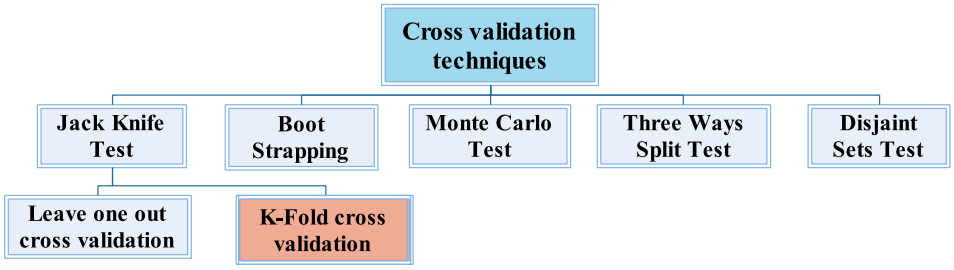

Fig. 3. Diagram of cross validation techniques types.

parameters of model [41–43]. The *K-fold* cross-validation is a technique of dividing the original sample randomly into *K* sub-samples. Then, a single sub-sample is regarded as the validation data for testing the model, and the remaining *K*-1 sub-samples are used as training data. These processes are repeated *K* times and each of the *K* sub-samples used exactly one as the validation data. The *K* results from the folds can then be averaged (or otherwise combined) to produce a single estimation. An example of estimating a turning parameter with *K-fold* cross-validation as follows [43]:

Step 1 Divide the data *K* roughly into equal parts;
Step 2 For each $i = 1, 2, 3, \ldots, K$ fit the model with parameter γ or other *K*-1 parts, giving $\alpha^{-k}(\gamma)$ and compute its error in predicting the *kth* part:

$$E_k(\gamma) = \sum_{i \in kth\ \text{part}} \left[y_i - x_i \alpha^{-k}(\gamma) \right]^2 \tag{5}$$

Step 3 Do this for many values of γ and choose the value of γ that makes smallest error. Fig. 4 shows the flowchart of *K*-fold cross validation.

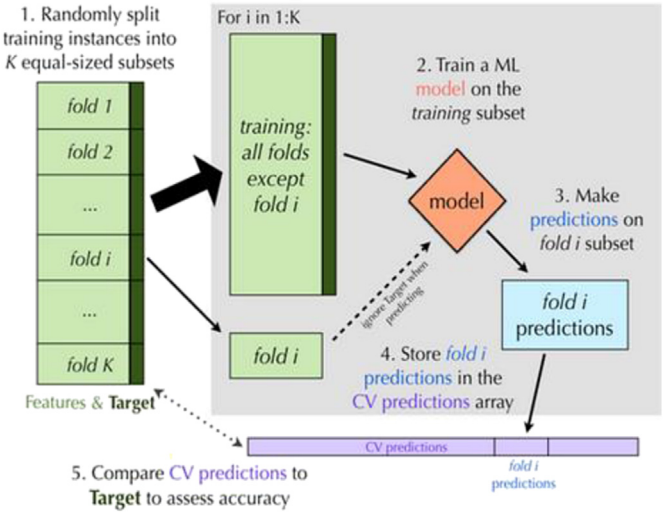

Fig. 4. Flowchart of the *K*-fold cross-validation [43].

2.4. Performance evaluation criteria

To evaluate the performance of the model, some criteria have been used from the literature. These criteria include: Root Mean Squared Error (RMSE), Mean Absolute Percentage Error (MAPE), and Model Efficiency (EF). These statistical parameters are defined as follows:

$$\mathrm{MAPE} = \frac{1}{n}\sum_{j=1}^{n}\left|\frac{d_j - p_j}{d_j}\right| \times 100 \tag{6}$$

$$\mathrm{RMSE} = \sqrt{\frac{\sum_{j=1}^{n}\left(d_j - p_j\right)^2}{n}} \tag{7}$$

$$\mathrm{EF} = \frac{\sum_{j=1}^{n}\left(d_j - \overline{d}\right)^2 - \sum_{j=1}^{n}\left(p_j - d_j\right)^2}{\sum_{j=1}^{n}\left(d_j - \overline{d}\right)^2} \tag{8}$$

$$R^2 = \left[\frac{\sum_{j=1}^{n}\left(d_j - \overline{d}\right)\left(p_j - \overline{p}\right)}{\sum_{j=1}^{n}\left(d_j - \overline{d}\right) \times \overline{\sum_{j=1}^{n}\left(p_j - \overline{p}\right)}}\right]^2 \tag{9}$$

where d_j is the *ith* component of the desired (actual) output for the *jth* pattern; p_j is the component of the predicted (fitted) output produced by the network for the *jth* pattern; $\overline{d}$ and $\overline{p}$ are the average of the whole desired (actual) and predicted output and n is the number of variable outputs. A model with the smallest RMSE, MAPE and largest EF is considered to be the best [44]. Finally, MATLAB software (Version 2013) used to solve the mathematical equations for GPR model.

3. Results and discussion

In this study, using the considered data sets and GPR model, an extensive exploration was performed to evaluate the influence of eight important input variables of N/N_s, T_{min}, T_{max}, T_{avg}, Rh, p and H_0 on prediction of daily horizontal global solar radiation (H) and then identify the most relevant sets of input parameters. For this purpose and also simplify the calculations, sensitivity analysis technique was used (Fig. 5). The current well-established sensitivity analysis methods can be classified into two categories: local and global techniques [45]. In this research, local sensitivity technique was selected and used. Local approaches estimate the effect of a single factor on the outputs while keeping all the others fixed at their nominal values. The result of this method shows in Table 1. The results of Table 1 show that N/N_s, T_{avg}, Rh and H_0 are the effective variables to predict daily horizontal global solar radiation at Mashhad city. At the second part, some different groups of data sets were used to select the best data collection to predict the horizontal global solar radiation (Table 1). As it can show, two data sets had the lowest error; (N/N_s- T_{avg}- Rh-H_0) and (N/Ns-T_{avg}-Rh-p-H_0). So the first group was selected, because it has fewer variables and also had proven by sensitivity analysis in the previous analysis.

Also, Table 1 shows the average and standard deviation of EF, R^2, MAPE and RMSE for all data include 100 different set with 5-fold cross validation and 20 repetitions (100 data set group). As it can show, the standard deviation of above statistical parameters (EF, R^2, MAPE, RMSE) is not zero, so the selective different data sets have a positive effect on predictive model performance.

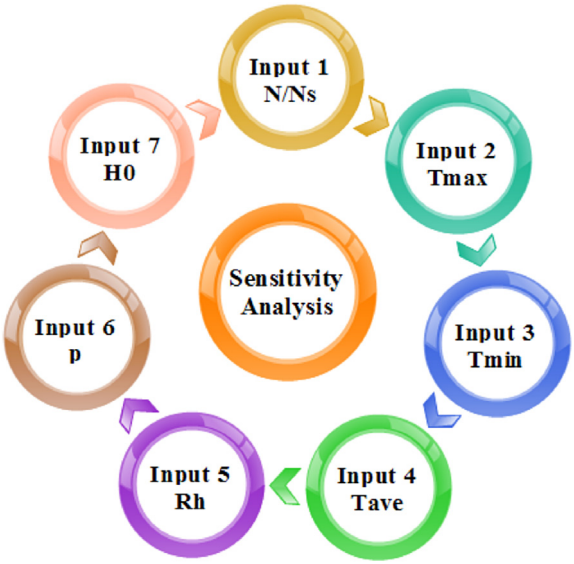

Fig. 5. Sensitivity analysis to select the important variables to predict daily horizontal global solar radiation at Mashhad city.

Application of sensitivity analysis was seen in a few researches. Alsina et al. [46], applied the ANN model to predict daily and monthly global solar radiation in Italy. They used Automatic Relevance Determination (ARD) Bayesian method as a sensitivity analysis to select the best and effective variables as the inputs for ANN model. This method creates an ordered list of the input by turning off one input at a time from the last to the first, sorting them by relevance. The results showed that the increase of the input number does not necessarily improve the performance of the ANN. The ARD method allows discarding irrelevant inputs (such as the longitude and the sunshine duration) that disturb the ANN training phase. The best results were for 7 input. The results of sensitivity analysis showed that, with ARD analysis and 7 inputs, the model had a MAPE of 1.67% and a maximum absolute percentage error of 8.42%, respectively; but, 66% and 10.14% for the method with all the 13 input. In another study Mostafavi et al. [47], developed a hybrid model by combining genetic programing (GP) with simulated annealing (SA) for global solar radiation estimation in two Iranian cities. They applied sensitivity analysis to assess the influence of maximum and minimum air temperature, relative humidity, precipitation and sunshine hours on global solar radiation prediction. Maximum and minimum air temperatures were found to be more relevant.

As it described, in this research, 100 data set groups was used to predict daily global solar radiation by GPR modal at Mashhad city. As we know, the performance of any model will change by changing in the data group, so the best data set was selected by attention to the results of training and testing of the GPR model (Table 2). From statistical point of view, both desired and predicted test data have been analyzed to determine whether there are statistically significant differences between them. The null hypothesis assumes that statistical parameters of both series are equal. *p* value was used to check each hypothesis. Its threshold value was 0.05. If *p* value is greater than the threshold, the null hypothesis is then fulfilled. To check the differences between the data series, different tests were performed and *p* value was calculated for each case.

The so called *t-test* was used to compare the means of both series. It was also assumed that the variance of both samples could be considered equal. The obtained *p* values were greater than the

Table 1
Results of sensitivity analysis for remove the ineffective variables to predict H parameter.

Model	Input variables	RMSE	MAPE	EF	R^2
All variables	N/N_s, T_{max}, T_{min}, T_{avg}, R_h, P,H_0	0.30 ± 0.06	5.15 ± 1.5	0.97 ± 0.00	0.97 ± 0.00
Sensitivity analysis	All-N/N_s	0.34 ± 0.09	5.78 ± 2.15	0.96 ± 0.01	0.96 ± 0.01
	All-T_{max}	0.30 ± 0.06	5.09 ± 1.59	0.97 ± 0.00	0.97 ± 0.00
	All-T_{min}	0.30 ± 0.00	5.19 ± 1.48	0.97 ± 0.00	0.97 ± 0.00
	All-T_{ave}	0.31 ± 0.07	5.19 ± 1.59	0.97 ± 0.00	0.97 ± 0.00
	All-Rh	0.32 ± 0.06	5.47 ± 1.56	0.97 ± 0.00	0.97 ± 0.00
	All-p	0.29 ± 0.07	4.88 ± 1.73	0.97 ± 0.00	0.97 ± 0.00
	All-H_0	0.43 ± 0.03	5.52 ± 0.87	0.97 ± 0.00	0.97 ± 0.00
Evaluate the other inputs	N/N_s, H_0	0.36 ± 0.00	6.28 ± 0.17	0.96 ± 0.00	0.96 ± 0.00
	T_{max}, T_{min}, H_0	0.32 ± 0.06	5.56 ± 1.39	0.97 ± 0.01	0.97 ± 0.01
	N/N_s, T_{max}, H_0	0.33 ± 0.05	5.81 ± 1.15	0.97 ± 0.00	0.97 ± 0.00
	N/N_s, Rh, H_0	0.34 ± 0.04	5.97 ± 1.05	0.97 ± 0.00	0.97 ± 0.00
	T_{max}, T_{min}, T_{ave}, H_0	0.31 ± 0.06	5.13 ± 1.20	0.97 ± 0.00	0.97 ± 0.00
	T_{max}, T_{min}, p, H_0	0.36 ± 0.08	6.11 ± 1.74	0.96 ± 0.01	0.96 ± 0.01
	N/Ns, Tmax, Tmin, Rh, H_0	0.32 ± 0.06	5.42 ± 1.43	0.97 ± 0.00	0.97 ± 0.00
	N/Ns, Tave, Rh, p, H_0	0.30 ± 0.07	4.97 ± 1.67	0.97 ± 0.00	0.97 ± 0.00
	N/Ns,Tave,Rh,H_0	0.30 ± 0.07	4.97 ± 1.67	0.97 ± 0.00	0.97 ± 0.00

Table 2
The *p*-value obtained from statistical comparisons between actual and predicted values for GPR model (the best data set extracted from *K-fold* analysis).

Phase	Criteria performance			p-value		
	EF	MAPE	RMSE	Distribution	Variance	Mean
Train	0.99	0.96	0.05	1.00	0.94	1.00
Test	0.97	6.01	0.33	1.00	0.72	1.00
Total	0.99	1.97	0.16	1.00	0.82	1.00

threshold; hence the null hypothesis cannot be rejected in all cases. The variance was analyzed using the *F-test*. Here, a normal distribution of samples was assumed. Again, the *p* values confirm the null hypothesis in all cases ($p > 0.72$). Finally, the *Kolmogorov–Smirnov test* also confirmed the null hypothesis. From statistical point of view, again, the *p* values confirm the null hypothesis in all cases. So the final results showed that the GPR model could predict daily solar radiation with high accuracy.

As it can see from Table 2, the criteria performance of training

Table 3
A literature review of solar radiation prediction (daily and monthly) by empirical, mathematical and soft computing models with statistical values.

References	Region	Model	RMSE	MAPE	R^2
[48]	Mumbai (India)	*ANN	3.64	3.02	0.85
[49]	Sharurha (Saudi Arabia)	*SVM	–	5.64	0.76
[50]	Varanasi (Indian)	ANN	0.35	1.36	–
[51]	China	Mathematical	3.77	–	0.76
[52]	Australia	Empirical	1.50	–	–
[53]	Canakkale (Turkey)	Mathematical and Empirical	0.34	–	–
[54]	Libya	ANN	–	–	0.98
[55]	India	Empirical	0.17	–	0.90
[34]	Tantakín (Turkey)	Empirical	2.60	12.32	0.76
[56]	Sari (Iran)	Empirical	5.14	–	0.86
[57]	Sokoto (Nigeria)	Empirical	0.92	–	0.86
[58]	Turkey	ANN	2.02	–	0.91
		*MLR	3.33	–	0.77
[59]	Isfahan (Iran)	SVM	2.00	10.45	0.91
[60]	Bandar Abbas (Iran)	SVM	1.43	6.99	0.97
[61]	Tabass (Iran)	ANFIS	0.89	3.96	0.99
[32]	Italy	ANN	0.03	5.72	0.99
[46]	Italy	ANN	–	1.67–4.25	–
[62]	China	ANN	0.87	–	0.97
		Mathematical	0.80–2.51	–	0.89–0.90
[63]	Zahedan and Bojnurd (Iran)	SVM	–	–	0.93
[64]	Bandar Abass (Iran)	*KELM	2.02	–	0.91
[65]	Kerman (Iran)	ANN	1.85	–	0.94
		ANFIS	1.84	–	0.93
		*GEP	1.89	–	0.93
[66]	Adana (Turkey)	ANN	–	2.81	0.99
[67]	Spain	ANN	0.05	–	–
[68]	Egypt	ANN	1.92	–	0.89
[62]	China	ANN	0.75	–	0.92
[69]	Turkey	ANN	–	10.53	0.98
[8]	Nigeria	ANN	–	11.45	0.97
[70]	South west of Iran	ANN	–	–	0.89
[71]	Portugal	ANN	11.68	5.10	–
[33]	Tehran (Iran)	ANN	0.05	1.5	0.99

Note: **ANN**: Artificial Neural Networks **KELM**: kernel extreme learning machine ANFIS: **Adaptive Neuro-Fuzzy Inference System GEP**: Gene Expression Programming **MLR**: Multilayer Regression.

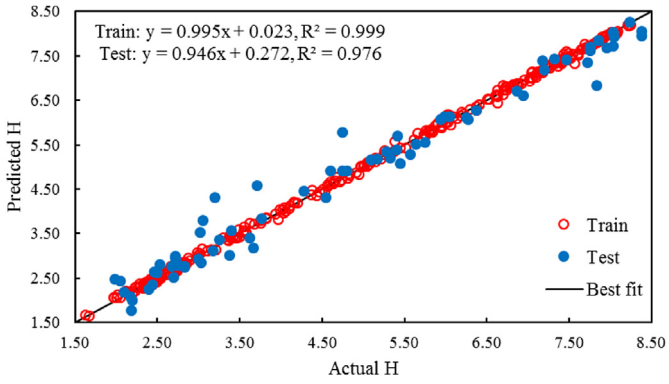

Fig. 6. The agreement between actual and predicted values by GPR model.

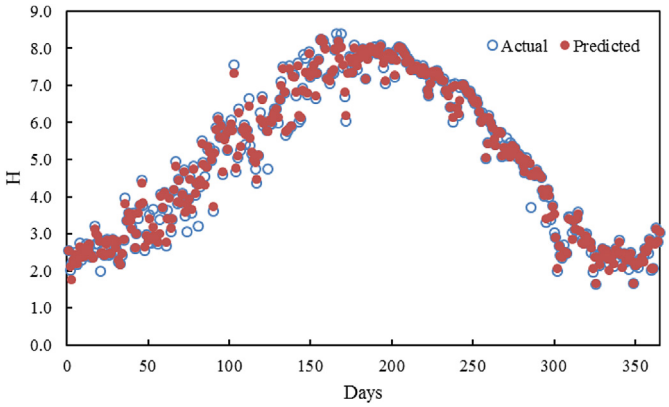

Fig. 7. Performance of GPR model to predict daily global solar radiation for all a year (365 day).

step is better than testing, but this result could not over train the model because MAPE, RMSE and EF for testing step are enough good and also the *p*-value showed that there is not any significant between the desired and predicted values. Finally in the training, validation and testing phases of GPR implementation, there is no significant difference between the actual data and the predicted data. Some similar researches and its results are shown in Table 3. As it can see, the presented GPR model has very good results according to MAPE and RMSE rather than other techniques.

Fig. 6 shows scattering the desired and predicted data by GPR model in both of training and testing steps with the selected data set group. As it can show, the correlation of determination (R^2) between desired and predicted data in training and testing steps are 0.999 and 0.976, respectively. Also, more than 97% of radiation data by selected model is around 45° line with a slope of near 1 and intercept of 0. So, these results can approve the ability of GPR model to predict daily global solar radiation with high accuracy. Fig. 7 shows the results of GPR model to predict all the daily global solar radiation for a year (365 day). As it can see, almost desired and predicted values are equal and conform with together.

Table 4 shows the performance of GPR model to predict the monthly global solar radiation by results of Table 2. Table 4 shows the average of daily solar estimation for each month. In this research, GPR model was evaluated from a statistical viewpoint for the first time. According to this perspective, the best model is obtained when the actual and predicted datasets are similar. The similarity of the datasets is assessed by mean equality (1), variance (2) and statistical distribution (3) tests. The statistical assumptions included in Eq. (10)–(12) were evaluated by paired *t*-test, F-test and Kolmogorov-Smirnov tests, respectively. The significance threshold was set at 0.05 for the assumptions. Thus, two datasets are equal when p-value > 0.05.

$$\begin{cases} H_0 : \overline{H}_a = \overline{H}_p \\ H_1 : \overline{H}_a \neq \overline{H}_p \end{cases} \tag{10}$$

$$\begin{cases} H_0 : \sigma^2_{Ha} = \sigma^2_{Hp} \\ H_1 : \sigma^2_{Ha} \neq \sigma^2_{Hp} \end{cases} \tag{11}$$

$$\begin{cases} H_0 : dis_{Ha} = dis_{Hp} \\ H_1 : dis_{Ha} \neq dis_{Ha} \end{cases} \tag{12}$$

where H_a and H_p represent the actual value of the daily global solar radiation on horizontal surface and the value predicted it by the model, and $\overline{H}_a$ and $\overline{H}_p$ denote their means, respectively. As it indicates, there is no significant between predicted and actual value of monthly solar radiation in all a year. The real interval of predicted and actual monthly solar radiation values is shown in Fig. 8.

Fig. 9 shows the standard deviation of parameter *H* for the year in Mashhad city. As it can see the standard deviation of parameter *H* in the first five months and the last quarter of the year is high, due to the relatively different atmospheric oscillation and instability in the studied area. This figure (Fig. 9) shows that the standard deviation of radiation in the first 5 months and the last quarter is higher than in other months. Therefore, it is expected that the trend of changes and fluctuations of *H* in these months will be higher. For solve this problem and also increase the ability of GPR model for actual application, we trained and selected a suitable model for every month.

Note: ANN: Artificial Neural Networks KELM: kernel extreme learning machine ANFIS: Adaptive Neuro-Fuzzy Inference System GEP: Gene Expression Programming MLR: Multilayer Regression.

Results are shown in Table 5. As it can see, the statistical performance indexes are almost equal to main model (Table 2) and improved than the results of Table 4. This result is one of the novelties of this research and can be used for application researches. Figs. 10 and 11 show the application of GPR model to predict daily and monthly solar radiation for 2009 to 2014.

Table 4
GPR model performance to predict monthly solar radiation at Mashhad city.

p-value			Criteria performance				p-value			Criteria performance			
Dist	Var	Ave	R^2	MAPE	RMSE	Month	Dist	Var	Ave	R^2	MAPE	RMSE	Month
0.94	0.66	0.75	0.93	1.01	1.05	July	1.00	0.92	0.80	0.75	7.33	0.68	January
1.00	0.94	0.92	0.95	1.28	1.16	August	0.78	0.72	0.97	0.94	5.55	0.90	February
1.00	0.83	0.86	0.98	1.79	1.15	September	0.94	0.53	0.83	0.90	8.04	1.95	March
1.00	0.89	0.77	0.95	4.69	1.55	October	1.00	0.48	0.96	0.97	3.06	1.31	April
1.00	0.87	0.85	0.97	4.12	0.40	November	0.76	0.28	0.90	0.88	4.41	3.57	May
1.00	0.85	0.95	0.93	4.91	0.42	December	0.78	0.45	0.78	0.93	2.22	2.08	June

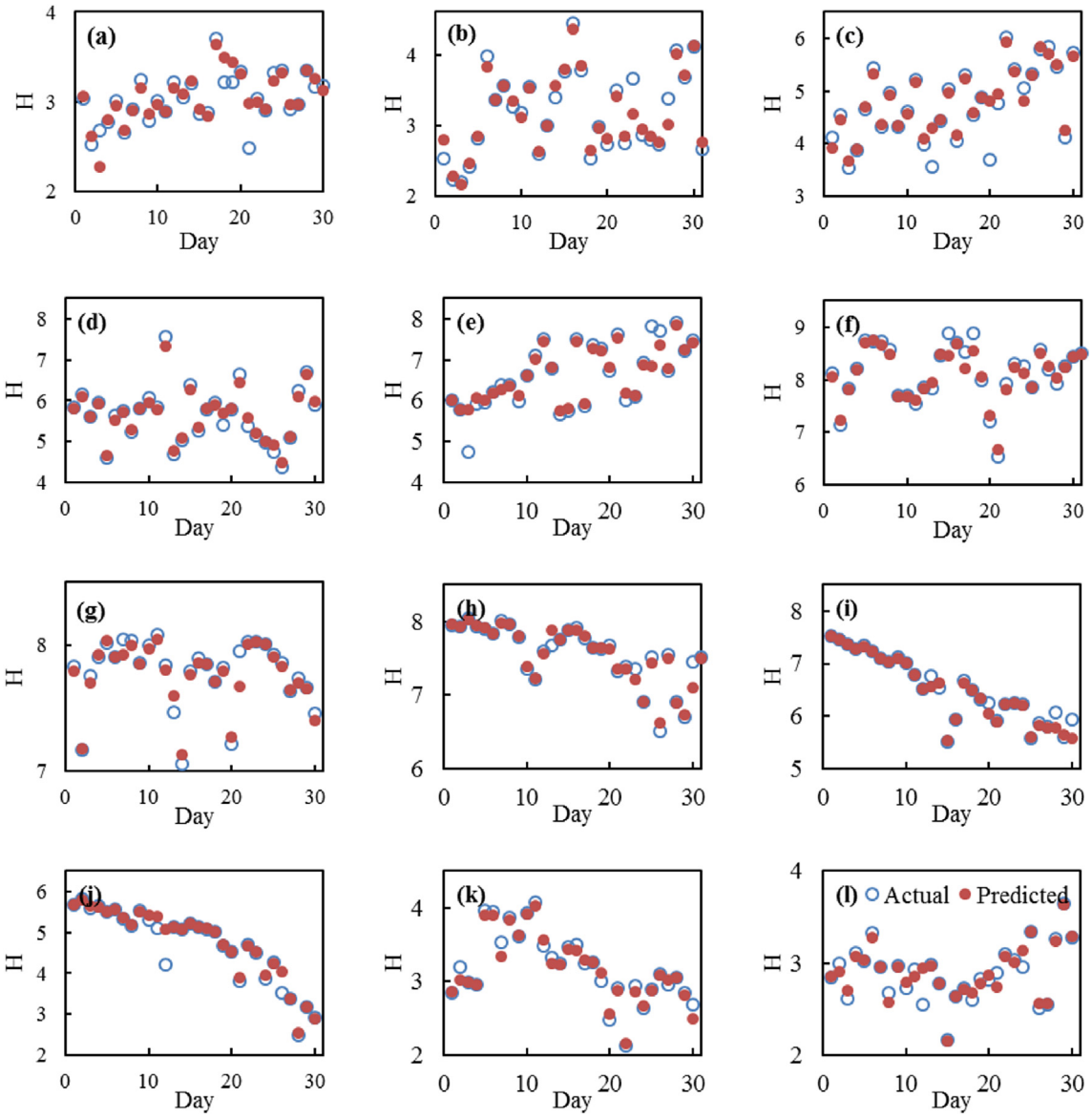

Fig. 8. Real interval of predicted and actual monthly solar radiation values for Mashhad city.

In order to assess the generalizability and stability of the GPR model, the *k-fold* cross validation with different sizes of training sets was used. The ratios of 80:20%, 60:40%, 40:60% and 20:80% were used as the size of the training and test data set. The data set using *a k-fold* cross validation was randomly divided into $k = 5$ parts (5-cross validation with 20 replications). In this way, 100 different data sets were generated for training and test phase. The mean and variance of the evaluation criteria such as RMSE, MAPE and R^2 were computed for each data set.

Based on this criterion, the best model was obtained when the variation of the mean and variance of the evaluation criteria (as a function of training data set size) were not too noticeable. The results are shown in Table 6. This table showed that by decreasing the training data set, RMSE and MAPE will increase and R^2 will decrease, respectively. The results of Table 6 show that if the GPR model having at least 60% of the total data, could make acceptable estimation of solar radiation in the whole year (both of train and test phase). This amount of training may vary for each model and study area. Therefore, it can be expected that the GPR model has good generalizability but it is recommended that for application researches to use more than 60% data for training step.

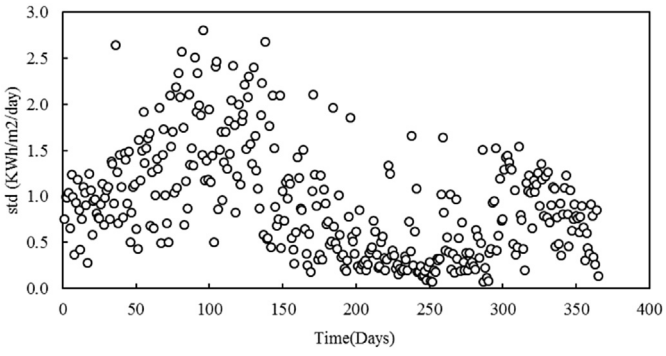

Fig. 9. Standard deviation of parameter *H* in the first five months and last quarter of the year in Mashhad city.

Table 5
GPR model performance for every month (specific model for each month).

p-value			Criteria performance				p-value			Criteria performance			
Dist	Var	Ave	R^2	MAPE	RMSE	Month	Dist	Var	Ave	R^2	MAPE	RMSE	Month
0.90	0.97	0.99	0.96	0.22	0.05	July	0.94	0.39	0.94	0.83	1.57	0.11	January
1.00	0.99	0.99	0.99	0.23	0.04	August	0.97	0.90	0.99	0.95	1.27	0.12	February
1.00	0.99	0.99	0.98	0.39	0.07	September	0.66	0.82	0.83	0.99	1.95	0.24	March
1.00	0.99	0.99	0.99	0.54	0.07	October	0.78	0.77	0.94	0.91	1.61	0.24	April
1.00	0.97	0.95	0.97	1.49	0.1	November	0.94	0.71	0.99	0.91	1.41	0.22	May
1.00	0.85	0.90	0.94	1.09	0.07	December	0.89	0.58	0.99	0.96	0.59	0.12	June

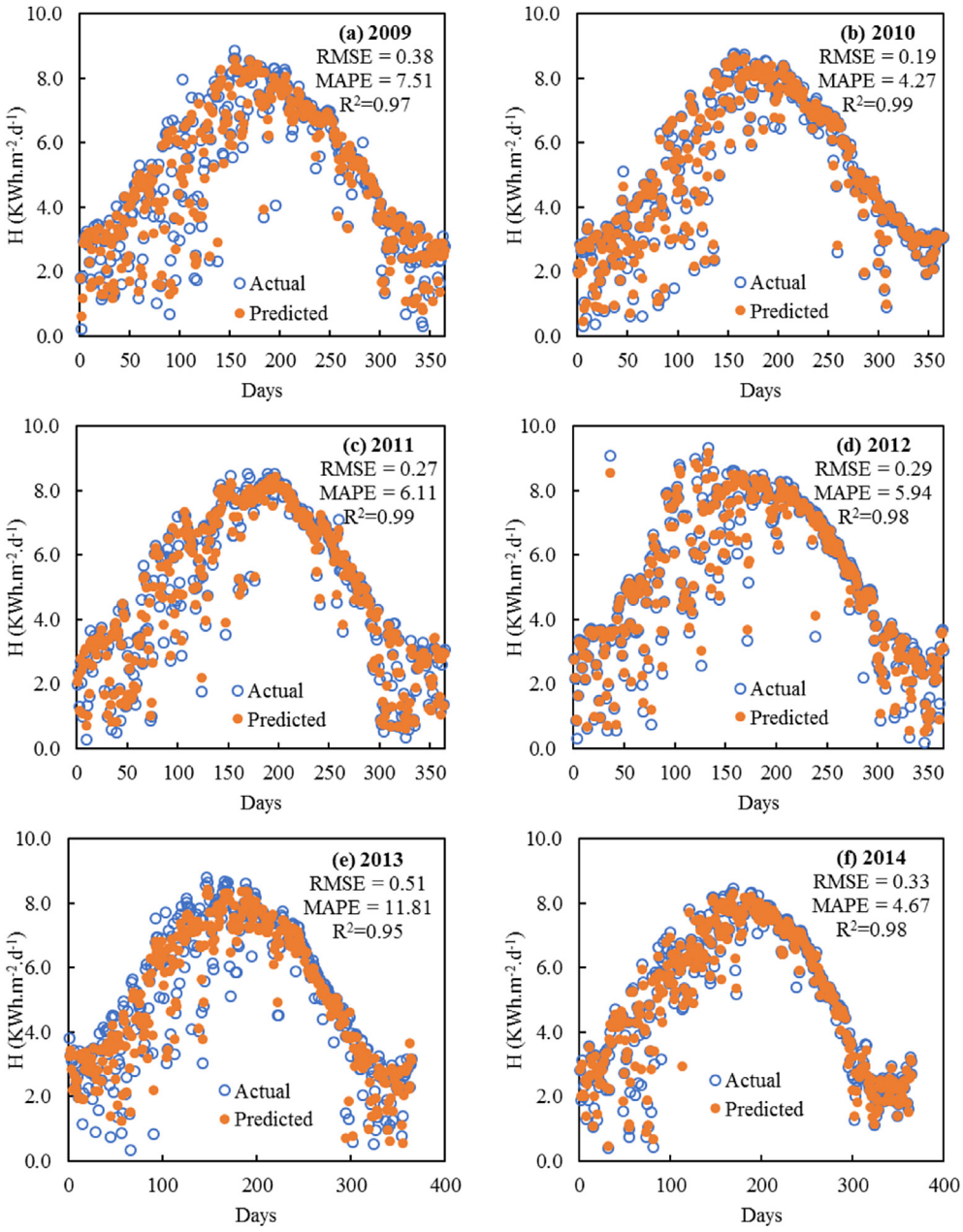

Fig. 10. Daily solar radiation forecasting by GPR model for 2009 (a) to 2014 (f) at Mashhad city.

4. Conclusion

In this paper, for the first time, Gaussian process regression (GPR) model was used to predict daily global solar radiation at Mashhad city, Iran. For evaluation the model, *5-fold* cross validation was used. Results showed that (N/N_s, T_{avg}, Rh, H_0) is the best data set group for evaluation the daily solar radiation at this region. Monthly evaluation from daily model showed that the

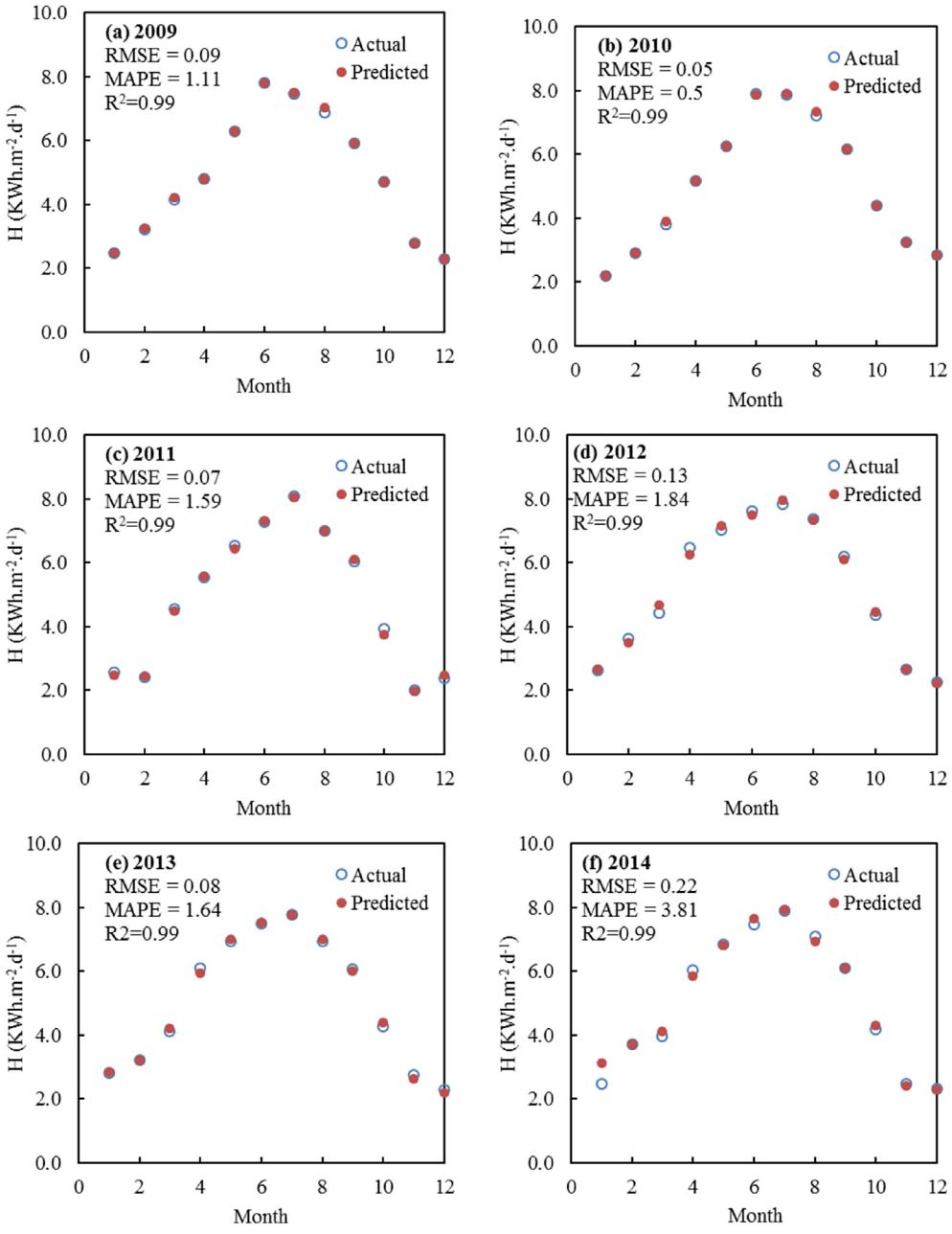

Fig. 11. Monthly solar radiation forecasting by GPR model for 2009 (a) to 2014 (f) at Mashhad city.

Table 6
5-fold cross validation analysis to select the best data training set.

	%	RMSE		MAPE		R^2	
		$\bar{x}\pm SD$	Best	$\bar{x}\pm SD$	Best	$\bar{x}\pm SD$	Best
Train	80	0.26 ± 0.12	0.05	4.57 ± 2.16	0.96	0.97 ± 0.01	0.99
	60	0.15 ± 0.13	0.06	2.62 ± 2.23	0.95	0.99 ± 0.01	0.99
	40	0.25 ± 0.12	0.34	4.59 ± 2.20	5.76	0.97 ± 0.01	0.97
	20	0.25 ± 0.12	0.31	4.47 ± 2.10	5.88	0.98 ± 0.01	0.98
Test	80	0.37 ± 0.04	0.33	6.57 ± 0.81	6.01	0.97 ± 0.00	0.97
	60	0.38 ± 0.02	0.33	6.68 ± 12.00	5.98	0.96 ± 0.00	0.97
	40	0.38 ± 0.02	0.36	6.71 ± 0.39	6.31	0.96 ± 0.00	0.97
	20	0.39 ± 0.02	0.37	7.04 ± 0.53	6.39	0.96 ± 0.00	0.97
Total	80	0.30 ± 0.07	0.16	4.97 ± 1.67	1.97	0.97 ± 0.01	0.99
	60	0.28 ± 0.04	0.21	4.24 ± 1.27	2.96	0.98 ± 0.00	0.99
	40	0.34 ± 0.02	0.35	5.86 ± 0.76	6.09	0.97 ± 0.00	0.97
	20	0.37 ± 0.01	0.36	6.53 ± 0.41	6.29	0.96 ± 0.00	0.97

main model is not suitable for every month because of temperature fluctuations and difference between climate situations in each month. So for every month, perfect model was trained and tested. Results showed that performance evaluation indexes of each model are better than main model. Generalizability and stability of the GPR model was evaluated by different sizes of training data (80, 60, 40 and 20% of total data). Results showed that GPR model can use with small size of data groups but for application research, it is recommended to use more than 60% of total data for training the model. Results of comparison between the GPR model and other soft computing models at literature review showed that this new model can use to predict daily and monthly solar radiation with high accuracy and useful for application researches especially in some parts of Iran and other developing countries.

Acknowledgments

The authors would like to thank the editor in chief and the anonymous referees for their valuable suggestions and useful comments that improved the paper content substantially. This study was supported by a grant from Ferdowsi University of Mashhad and Ramin Agriculture and Natural Resources University of Khuzestan, Iran. The authors are grateful for the support provided by these Universities.

References

[1] M. Taki, Y. Ajabshirchi, S.F. Ranjbar, A. Rohani, M. Matloobi, Heat transfer and MLP neural network models to predict inside environment variables and energy lost in a semi-solar greenhouse, Energy Build. 110 (2016) 314–329.
[2] G.E. Hassan, M.E. Youssef, M.A. Ali, Z.E. Mohamad, A.L. Shehata, Performance assessment of different day-of-the-year-based models for estimating global solar radiation - case study: Egypt, J. Atmos. Sol. Terr. Phys. 149 (2016a) 69–80.
[3] A.A. El-Sebaii, F.S. Al-Hazmi, A.A. Al-Ghamdi, S.J. Yaghmour, Global, direct and diffuse solar radiation on horizontal and tilted surfaces in Jeddah, Saudi Arabia, Appl. Energy 87 (2010) 568–576.
[4] J. Piri, O. Kisi, Modeling solar radiation reached to the Earth using ANFIS, NN-ARX, and empirical models (Case studies: Zahedan and Bojnurd stations), J. Atmos. Sol. Terr. Phys. 123 (2015) 39–47.
[5] S. Sharifi, V. Rezaverdinejad, V. Nourani, Estimation of daily global solar radiation using wavelet regression, ANN, GEP and empirical models: a comparative study of selected temperature-based approaches, J. Atmos. Sol. Terr. Phys. 149 (2016) 131–145.
[6] B. Amrouche, X. Le Pivert, Artificial neural network based daily local forecasting for global solar radiation, Appl. Energy 130 (2014) 333–341.
[7] H. Li, W. Ma, Y. Lian, X. Wang, Estimating daily global solar radiation by day of year in China, Appl. Energy 87 (2010) 3011–3017.
[8] D.A. Fadare, Modelling of solar energy potential in Nigeria using an artificial neural network model, Appl. Energy 86 (2009) 1410–1422.
[9] C. Voyant, C. Darras, M. Muselli, C. Paoli, M.L. Nivet, P. Poggi, Bayesian rules and stochastic models for high accuracy prediction of solar radiation, Appl. Energy 114 (2014) 218–226.
[10] G.E. Hassan, M.E. Youssef, Z.E. Mohamed, M.A. Ali, A.A. Hanafy, New temperature-based models for predicting global solar radiation, Appl. Energy 179 (2016b) 437–450.
[11] L. Olatomiwa, S. Mekhilef, S. Shamshirband, K. Mohammadi, D. Petrovic, C. Sudheer, A support vector machine–firefly algorithm-based model for global solar radiation prediction, Sol. Energy 115 (2015a) 632–644.
[12] K. Mohammadi, S. Shamshirband, A. Kamsin, P.C. Lai, Z. Mansor, Identifying the most significant input parameters for predicting global solar radiation using an ANFIS selection procedure, Renew. Sustain. Energy Rev. 63 (2016) 423–434.
[13] L. Wang, O. Kisi, M.Z. Kermani, G.A. Salazar, Z. Zhu, W. Gong, Solar radiation prediction using different techniques: model evaluation and comparison, Renew. Sustain. Energy Rev. 61 (2016) 384–397.
[14] S. Shamshirband, K. Mohammadi, H.U. Chen, G.N. Samy, D. Petkovic, C. Ma, Daily global solar radiation prediction from air temperatures using kernel extreme learning machine: a case study for city of Bandar Abass, Iran, J. Atmos. Sol. Terr. Phys. 75 (2016a) 415–423.
[15] A.S.S. Dorvlo, J.A. Jervase, A. Al-Lawati, Solar radiation estimation using artificial neural networks, Appl. Energy 71 (2002) 307–319.
[16] A.K. Yadav, H. Malik, S.S. Chandel, Application of rapid miner in ANN based prediction of solar radiation for assessment of solar energy resource potential of 76 sites in Northwestern India, Renew. Sustain. Energy Rev. 52 (2015) 1093–1106.
[17] L. Olatomiwa, S. Mekhilef, S. Shamshirband, D. Petovic, Adaptive neuro-fuzzy approach for solar radiation prediction in Nigeria, Renew. Sustain. Energy Rev. 51 (2015b) 1784–1791.
[18] A. Teke, H.B. Yildrim, O. Celik, Evaluation and performance comparison of different models for the estimation of solar radiation, Renew. Sustain. Energy Rev. 50 (2015) 1097–1107.
[19] M.A. Shamim, R. Remean, M. Bray, D. Han, An improved technique for global solar radiation estimation using numerical weather prediction, J. Atmos. Sol. Terr. Phys. 129 (2015) 13–22.
[20] A. Razmjoo, S.M. Heibati, M. Qolipour, E.S. Al kath ir, A. Faraji, Estimating of monthly global solar radiation by Angstrom- prescott (A-P) method for Ahvaz and abadan cities, Int. J. Renew. Energy Technol. Res. 5 (2) (2016) 1–13.
[21] S. Jovic, O. Anicic, M. Marsenic, B. Nedic, Solar radiation analyzing by neuro-fuzzy approach, Energy Build. 129 (2016) 261–263.
[22] R. Kumar, R.K. Aggarwal, J.D. Sharma, Comparison of regression and artificial neural network models for estimation of global solar radiations, Renew. Sustain. Energy Rev. 52 (2015) 1294–1299.
[23] S. Mohanty, P.K. Patra, S.S. Sahoo, Prediction and application of solar radiation with soft computing over traditional and conventional approach – a comprehensive review, Renew. Sustain. Energy Rev. 65 (2016) 778–796.
[24] V.H. Quej, J. Almorox, A. Arnaldo, L. aito, ANFIS, SVM and ANN soft-computing techniques to estimate daily global solar radiation in a warm sub-humid environment, J. Atmos. Sol. Terr. Phys. 155 (2017) 62–70.
[25] Fariba Besharat, A. Dehghan Ali, R. Faghih Ahmad, Empirical models for estimating global solar radiation: a review and case study, Renew. Sustain. Energy Rev. 21 (2013) 798–821.
[26] Suehrcke Harry, S. Bowden Ross, K.G.T. Hollands, Relationship between sunshine duration and solar radiation, Sol. Energy 92 (2013) 160–171.
[27] Selmin Ener Rusen, Annette Hammer, G. Bulent, Estimation of daily global solar irradiation by coupling ground measurements of bright sun shine hours to satellite imagery, Energy 58 (2013) 417–425.
[28] Notton Gilles, Paoli Christophe, Ivanova Liliana, Vasileva Siyana, Nivet Marie Laure, Neural network approach to estimate10-min solar global irradiation values on tilted planes, Renew. Energy 50 (2013) 576–584.
[29] Voyant Cyril, Muselli Marc, Paoli Christophe, Marie-Laure Nivet, Hybrid methodology for hourly global radiation forecasting in Mediterranean area, Renew. Energy 53 (2013) 1–11.
[30] X. Yu, Z. Wu, W. Jiang, X. Guo, Predicting daily photosynthetically active radiation from global solar radiation in the Contiguous United States, Energy Convers. Manag. 89 (2015) 71–82.
[31] F.J.L. Lima, F.R. Martins, E.B. Pereira, E. Lorenz, D. Heinemann, Forecast for surface solar irradiance at the Brazilian Northeastern region using NWP model and artificial neural networks, Renew. Energy 87 (2016) 807–818.
[32] C. Renno, F. Petito, A. Gatto, Artificial neural network models for predicting the solar radiation as input of a concentrating photovoltaic system, Energy Convers. Manag. 106 (2015) 999–1012.
[33] M. Vakili, S.R. Sabbagh-Yazdi, S. Khosrojerdi, K. Kalhor, Evaluating the effect of particulate matter pollution on estimation of daily global solar radiation using artificial neural network modeling based on meteorological data, J. Clean. Prod. 141 (2017) 1275–1285.
[34] V.H. Quej, J. Almorox, M. Ibrakhimov, L. Saito, Empirical models for estimating daily global solar radiation in Yucatán Peninsula, Mexico, Energy Convers. Manag. 110 (2016) 448–456.
[35] R. Yacef, M. Benghanem, A. Mellit, Prediction of daily global solar irradiation data using Bayesian neural network: a comparative study, Renew. Energy 48 (2012) 146–154.
[36] L. Zou, L. Wang, A. Lin, Estimation of global solar radiation using an artificial neural network based on an interpolation technique in southeast China, J. Atmos. Sol. Terr. Phys. 146 (2016) 110–122.
[37] S. Shamshirband, K. Mohammadi, H.L. Chen, G.N. Samy, D. Petkovic, C. Ma, Daily global solar radiation prediction from air temperatures using kernel extreme learning machine: a case study for Iran, J. Atmos. Sol. Terr. Phys. 134 (2015) 109–117.
[38] M. Kottek, J. Grieser, C. Beck, B. Rudolf, F. Rubel, World map of the Koppen–Geiger climate classification updated, Meteorol. Z 15 (3) (2005) 259–263.
[39] Z.Y. Wan, P.S. Sapsis, Reduced-space Gaussian Process Regression for data-driven probabilistic forecast of chaotic dynamical systems, Phys. D. 345 (2017) 40–55.
[40] C.E. Rasmussen, C.K.I. Williams, Gaussian Processes in Machine Learning, The MIT Press, Cambridge, MA, 2005.
[41] T.F. Tvedskov, T.J. Meretoja, M.B. Jensen, M. Leidenius, N. Kroman, Cross-validation of three predictive tools for non-sentinel node metastases in breast cancer patients with micrometastases or isolated tumor cells in the sentinel node, Eur. J. Surg. Oncol. 40 (2013) 435–441.
[42] C. Shaoa, K. Paynabarb, T.H. Kima, J.H. Jinc, S.J. Hu, J.P. Spicerd, H. Wangd, J.A. Abelld, Feature selection for manufacturing process monitoring using cross-validation, J. Manuf. Syst. 32 (2013) 550–555.
[43] P. Jiang, J. Chen, Displacement prediction of landslide based on generalized regression neural networks with K-fold cross-validation, Neurocomputing (2016), http://dx.doi.org/10.1016/j.neucom.2015.08.118.
[44] A. Das, J. Park, J. Park, Estimation of available global solar radiation using sunshine duration over South Korea, J. Atmos. Sol. Terr. Phys. 134 (2015) 22–29.
[45] L. Chen, G. Yan, W. Tianxing, H. Ren, J. Calbo, J. Zhao, R. Mckenzie, Estimation of surface shortwave radiation components under all sky conditions: modeling and sensitivity analysis, Remote Sens. Environ. 123 (2012) 457–469.
[46] E.F. Alsina, M. Bortolini, M. Gamberi, A. Regattieri, Artificial neural network optimization for monthly average daily global solar radiation prediction, Energy Convers. Manag. 120 (2016) 320–329.
[47] E.S. Mostafavi, S. Saeidi Ramiyani, R. Sarvar, H. Izadi Moud, S.M. Mousavi, A hybrid computational approach to estimate solar global radiation: empirical evidence from Iran, Energy 49 (2013) 204–210.
[48] P. Neelamegam, V.A. Amirtham, Prediction of solar radiation for solar systems by using ANN models with different back propagation algorithms, J. Appl. Res. Technol. 14 (2016) 206–214.
[49] J.M. Bakhashwain, Prediction of global solar radiation using support vector machines, Int. J. Green Energy 13 (14) (2016) 1467–1472.
[50] N. Kumar, S.P. Sharma, U.K. Sinha, Y. Nayak, Prediction of solar energy based on intelligent ANN modeling, Int. J. Renew. Energy Res. 6 (1) (2016) 183–188.
[51] X. Xu, H. Du, G. Zhou, F. Mao, P. Li, W. Fan, D. Zhu, A method for daily global solar radiation estimation from two instantaneous values using MODIS atmospheric products, Energy 111 (2016) (2016) 117–125.
[52] N. Lockart, D. Kavetski, S.W. Franks, A new stochastic model for simulating

daily solar radiation from sunshine hours, Int. J. Climatol. 35 (6) (2014) 1090–1106.
[53] E. Akarslan, F.O. Hocaoglu, A novel adaptive approach for hourly solar radiation forecasting, Renew. Energy 87 (2016) 628–633.
[54] Kutucu, H., Almryad, A, 2016, Modeling of Solar Energy Potential in Libya using an Artificial Neural Network Model, IEEE First International Conference on Data Stream Mining & Processing, 23–27 August, Lviv, Ukraine.
[55] S. Kirmani, M. Jamil, M. Rizwan, Empirical correlation of estimating global solar radiation using meteorological parameters, Int. J. Sustain. Energy 34 (5) (2015) 327–339.
[56] G. Ghobadi, B. Gholizadeh, S. Motavalli, Estimation global solar radiation from common metrological data in Sari station, Iran, Int. J. Agric. Crop Sci. 5 (21) (2013) 2650–2654.
[57] M.S. Okundamiya, J.O. Emagbetere, E.A. Ogujor, Evaluation of various global solar radiation models for Nigeria, Int. J. Green Energy 13 (5) (2016) 505–512.
[58] M. Sahin, Y. Kaya, Uyar, Comparison of ANN and MLR models for estimating solar radiation in Turkey using NOAA/AVHRR data, Adv. Space Res. 51 (2013) 891–904.
[59] K. Mohammadi, S. Shamshirband, M.H. Anisi, K.A. Alam, D. Petkovic, Support vector regression based prediction of global solar radiation on a horizontal surface, Energy Convers. Manag. 91 (2015a) 433–441.
[60] K. Mohammadi, S. Shamshirband, C.W. Tong, M. Arif, D. Petkovic, S. Ch, A new hybrid support vector machine–wavelet transform approach for estimation of horizontal global solar radiation, Energy Convers. Manag. 92 (2015b) 162–171.
[61] K. Mohammadi, S. Shamshirband, C.W. Tong, K.A. Alam, D. Petkovic, Potential of adaptive neuro-fuzzy system for prediction of daily global solar radiation by day of the year, Energy Convers. Manag. 93 (2015c) 406–413.
[62] Y. Jiang, Computation of monthly mean daily global solar radiation in China using artificial neural networks and comparison with other empirical models, Energy 34 (2009) 1276–1283.
[63] J. Piri, S. Shamshirband, D. Petkovic, C.W. Tong, M.H. Rehman, Prediction of the solar radiation on the Earth using support vector regression technique, Infrared Phys. Technol. 14 (2014) 1350–4495.
[64] S. Shamshirband, K. Mohammadi, H. Khorasanizadeh, L.P. Yee, M. Lee, D. Petovic, E. Zalnezhad, Estimating the diffuse solar radiation using a coupled support vector machine–wavelet transform model, Renew. Sustain. Energy Rev. 56 (2016b) 428–435.
[65] S. Mehdizadeh, J. Behmanesh, K. Khalili, Comparison of artificial intelligence methods and empirical equations to estimate daily solar radiation, J. Atmos. Sol. Terr. Phys. 146 (2016) 215–227.
[66] O. Çelik, A. Teke, B. Yildrim, The optimized artificial neural network model with Levenberg- Marquardt algorithm for global solar radiation estimation in eastern mediterranean region of Turkey, J. Clean. Prod. 10 (1–12) (2016).
[67] J. Almorox, C. Hontoria, Global solar radiation estimation using sunshine duration in Spain, Energy Convers. Manag. 45 (9–10) (2004) 1529–1535.
[68] A.A.E. Sebaii, A.A. Trabea, Estimation of horizontal diffuse solar radiation in Egypt, Energy Convers. Manag. 44 (15) (2003) 2471–2482.
[69] A. Sozen, E. Arcaklioğlu, M. Ozalp, Estimation of solar potential in Turkey by artificial neural networks using meteorological and geographical data, Energy Convers. Manag. 45 (2004) 3033–3052.
[70] A. Rahimikhoob, Estimating global solar radiation using artificial neural network and air temperature data in a semi-arid environment, Renew. Energy 35 (2010) 2131–2135.
[71] J. Faceira, P. Afonso, P. Salgado, Prediction of solar radiation using artificial neural networks, in: Proceedings of the 11th Portuguese Conference on Automatic Control, 2015, pp. 397–406.